JOURNAL OF SOLID STATE CHEMISTRY 113, 373–378 (1994)

Crystal Structure of Sr-Substituted Hydroxyapatite Synthesized by Hydrothermal Method

Masanori Kikuchi,[1] Atsushi Yamazaki, and Ryohei Otsuka

Department of Mineral Resources Engineering, School of Science and Engineering, Waseda University, 3-4-1 Okubo, Shinjuku-ku, Tokyo 160, Japan

and

Masaru Akao and Hideki Aoki

Division of Inorganic Materials, Institute for Medical and Dental Engineering, Tokyo, Medical and Dental University, 2-3-10 Kanda-surugadai, Chiyoda-ku, Tokyo, 101 Japan

Received November 15, 1993; in revised form April 5, 1994; accepted April 12, 1994

Single crystals of Sr-substituted hydroxyapatite, $(Ca_{9.42}Sr_{0.18}H_{0.8}(PO_4)_6(OH)_2$, up to 0.2 × 0.2 × 5 mm³ maximum size were grown hydrothermally from calcium hydrogenphosphate ($CaHPO_4$) and strontium hydrogenphosphate ($SrHPO_4$) in a long tube-type autoclave using a temperature gradient technique. The single crystals, containing 1.92 mole% Sr to (Ca + Sr) and having a (Ca + Sr)/P atomic ratio of 1.60, had a hexagonal–prismatic shape with density of 3.207 g/cm³. The crystal had a hexagonal system, space group $P6_3/m$ with $a = 9.3920(7)$ Å, $c = 6.890(1)$ Å, and $Z = 1$. A hexagonal–prismatic crystal, 165 × 165 × 231 μm³ in size, was used for crystal structure refinement. The atomic parameters in $P6_3/m$ were refined to $R = 5.9\%$ and $R_wÅ = 6.3\%$ with 2018 independent reflections. The preferential substitution site of Sr for Ca was determined as the Ca(1) site.

1. INTRODUCTION

Hydroxyapatite, $Ca_{10}(PO_4)_6(OH)_2$, in nature includes Sr, Ba, Fe, etc. as impurities of Ca ions. Among these elements, Sr substitution has been studied in the mineralogical and biological fields because of its similarity to Ca in chemical properties. The effect of exercise on strength and Sr substitution of rat femur bone was studied by Aoki *et al.* (1). The Sr/Ca ratio in femur bone of an exercise group of rats increased compared with that of a control group. The effect of Sr uptakes on the solubility of powdered tooth enamel was studied by Gedalia *et al.* (2). With an increase in the Sr amount, the solubility of powdered enamel was increased. Powder of Sr-substituted hydroxyapatite was synthesized by Collin (3, 4) using the wet method and by Lagergren and Calström (5) using a solid-state reaction. From the powder studies, the cell parameters of Sr-substituted hydroxyapatite were extended proportionally with an increase in substituted Sr amounts. On the other hand, Sr-substituted hydroxyapatite was synthesized by Kikuchi *et al.* (6). They concluded that the Sr- to Ca-site ratio in hydrothermally synthesized Sr-substituted hydroxyapatite was not beyond 40 mole%, which was equal to the Ca(1)-site to Ca-site ratio, and the cell expansion of Sr-substituted hydroxyapatite was not proportional to the Sr substitution amount. Single crystals of Sr-substituted chlorapatite were synthesized by a flux technique, and their crystal structure was refined by Sudarsanan and Young (7). They concluded that Sr ions were substituted preferentially at the Ca(2) site. The preferential substitution site of Sr for natural Sr-substituted fluorapatite as the Ca(2) site was determined by Hughes *et al.* (8). However, the crystal structure of Sr-substituted hydroxyapatite has not been refined by any workers.

In this paper, the crystal structure of hydrothermally grown Sr-substituted hydroxyapatite is described. Further, the preferential substitution site of Sr for Ca is determined.

2. MATERIALS AND METHODS

2.1. Hydrothermal Synthesis of Sr-Substituted Hydroxyapatite Single Crystals

Single crystals of Sr-substituted hydroxapatite were grown hydrothermally from calcium and strontium hydrogenphosphates by gradual heating with a temperature gradient. The experimental setup is shown in Fig. 1; the volume of the autoclave is 1000 cm³. The experimental

[1] To whom correspondence should be addressed.

0022-4596/94 $6.00

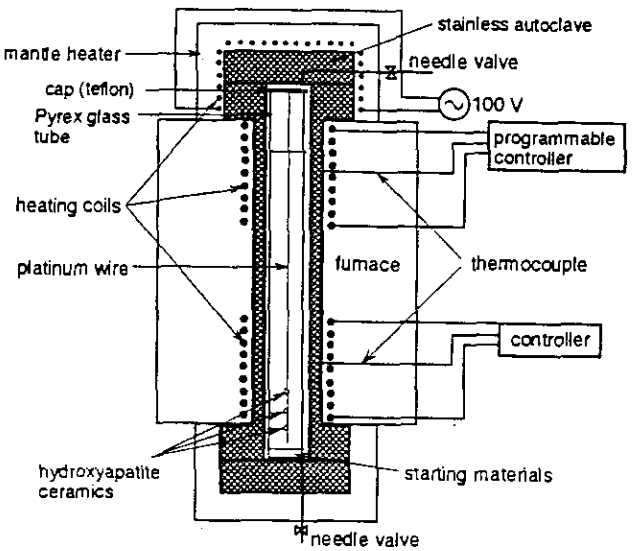

FIG. 1. Experimental setup of autoclave with a two-zone furnace.

conditions of the single crystal growth were as follows: The starting materials, weighted out 44.1 mmole at 2/8 of the Sr/Ca atomic ratio and 594 cm^3 of distilled water, were put into a Pyrex glass reaction tube. Resulting from preliminary runs (6), the single crystals of Sr-substituted hydroxyapatite grew at a low pH. Consequently, to control the final pH value to low pH area, the pH value of the starting aqueous solution was controlled at pH 2.0 by adding 6 cm^3 of 1.73 M orthophosphoric acid aqueous solution. Sintered hydroxyapatite ceramic disks $10\phi \times 4$ mm^3 in size, hung from a teflon cap with a platinum wire to reach 6, 9, or 12 cm from the bottom, were used as seeds. The Pyrex glass reaction tube was inserted into the autoclave, the filling ratio being 60%. The upper heater was controlled by programmable controller RTC-5130 (Ohkura Denki Co., Ltd.). The lower heater was controlled by SR10 (Shimaden Co., Ltd.).

The upper and lower heaters were immediately heated to 523 and 493 K, respectively. The upper mantle heater also was heated to 693 K. After 6 hr holding, the upper heater was heated to 603 K at a heating rate of 0.01 K/min. The observed pressure at 603 K was 40.2 MPa. The temperature distributions of the autoclave are shown in Fig. 2. Six days after aging at 603 K, high-pressure steam was released from the bottom needle valve, and the reaction tube was taken out from the bottom of the autoclave. The seed crystals were taken out, and precipitates in the tube were filtrated. The pH value of the filtrate was measured with a digital pH meter at room temperature 24 hr after filtration. Single crystals were picked up from the seeds, wire, and precipitates.

The single crystals obtained were identified by the X-ray powder diffraction method with the PW-1820 system (Nihon Philips Co.) using CuK_α radiation, and cell parameters were calculated from 11 peaks measured with an X-ray diffractometer by the least-squares method using program RLC-3 (9). Silicon powder (NBS-640) was used as an internal standard. The density of the single crystals was measured by the heavy-liquid method using methylene iodide and tetrachlorethane as heavy liquids. Chemical analysis of the single crystals was carried out by wavelength-dispersive X-ray spectroscopy and energy-dispersive X-ray spectroscopy using $CaSiO_3$, $SrTiO_3$, and GaP as standards with JXA733 (JEOL Co., Ltd.) and TN-5400 (Tracor Northern Co., Ltd.). Forms and optical properties of the crystals were observed using a polarizing microscope. The elongated axis of the crystals were determined by an X-ray camera technique. The infrared spectrum of the crystals was measured with an I-2000 infrared spectrometer (Hitachi Co., Ltd.) using the KBr disk technique.

2.2. *Crystal Structure Refinement of Sr-Substituted Hydroxyapatite*

The single crystal used for crystal structure refinement was hexagonal–prismatic in form and $165 \times 165 \times 231$ μm^3 in size. The space group was determined by the Weissenberg camera technique. The intensities were measured with an AFC5R four-circle diffractometer (Rigaku Co., Ltd.) using graphite-monochromatized MoK_α radiation at 150 kV and 150 mA and a ω-2θ scan technique at a scan rate of 4°/min. A total of 2018 independent reflection data ($|F_o| > 3\sigma(|F_o|)$) were collected

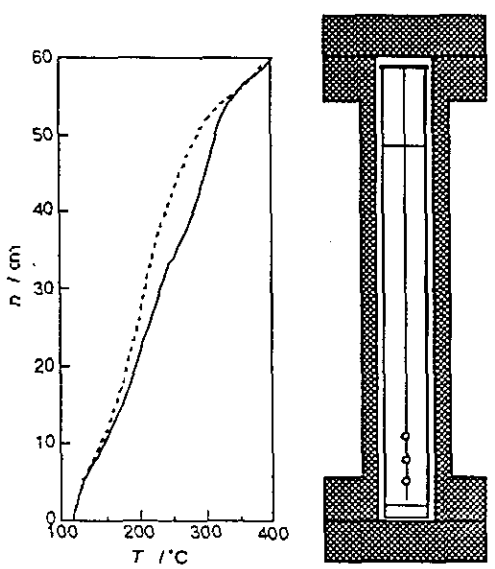

FIG. 2. Temperature distributions in autoclave. (Dashed and solid lines indicate the temperature in the autoclave at 220–250°C and 220–330°C of lower–upper heater temperatures, respectively.)

TABLE 1
Chemical Composition of Sr-Substituted Hydroxyapatite

Ca	34.96(5) wt.%
Sr	1.43(6) wt.%
P	17.29(5) wt.%
M/P	1.60
Sr/*M*	1.92 mol.%

Note. *M*: Ca + Sr.

within the range of $2\theta \leq 120°$ at 293 K. The intensities were corrected for Lorentz and polarization factors. Absorption corrections were not made. The atomic scattering factors for ions and the anomalous dispersion factors were taken from (10). For the O^{2-} ion, atomic scattering factors were taken from the work of Tokonami (11), and atomic scattering factors of P^{5+} were taken from (12). In this calculation, we considered the scattering factors for OH^- to be those of O^-. The weighing scheme for the observed amplitudes was $w = 1/(a + bF_o + cF_o^2 + dF_o^3)$, where a, b, c, and d were varied so that $w(F_o - F_c)^2$ was independent of the magnitude of F_o. The values of a, b, c, and d in the last cycle were 21.169, 1.1967×10^{-1}, -3.5767×10^{-4}, and 7.1524×10^{-6}, respectively. At first, starting from the positional parameters of Ca–hydroxyapatite (13), the atomic parameters without hydrogen atoms were refined in space group $P6_3/m$, considering substitution of Sr for Ca by the full-matrix least-squares program LINUS (14). Afterward, a site analysis was carried out as follows: The atomic parameters were refined using populations of Ca, Sr, and O as variables under limited vacancy and electrical charge balance with permission of free distributions of Sr ions between the Ca(1) and Ca(2) site (i), with the Sr population being calculated from EPMA data and fixed Sr position to the Ca(1) site (ii) and Ca(2) site (iii). From R-factors obtained, Hamilton's R-factor significant test (15) was carried out for (i)–(iii).

3. RESULTS AND DISCUSSION

3.1. Hydrothermal Synthesis of Sr-Substituted Hydroxyapatite Single Crystals

The area of single crystal growth was about 36–38 cm from the bottom of the tube. The temperatures in this area were 538–543 K and indicated maximum temperature shift. No large crystals were grown on the seed crystals, and the sintered hydroxyapatite disks (seed) themselves were dissolved. These results suggested that at pH 2.0, dissolution of the starting materials and hydroxyapatite occurred within a low-temperature range, and the hydroxyapatite was recrystallized within a high-temperature range.

The single crystals obtained up to $0.2 \times 0.2 \times 5$ mm^3 in size were identified as hydroxyapatite by the X-ray powder diffraction method, and cell parameters were a = 9.3920(7) Å and c = 6.890(1) Å. These values were nearly equal to the values of JCPDS 9-432 within 0.3% error. The results indicated that only a few Sr ions were substituted in the hydroxyapatite single crystals. The density of the single crystals was determined to be 3.207(1) g/cm^3. The result of chemical analysis by wavelength-dispersive X-ray spectroscopy is shown in Table 1. These ratios were calculated using ZAF correction. The (Ca + Sr)/P atomis ratio of the crystal was 1.60, and the Sr/(Ca + Sr) atomic ratio was 1.92 mole%. These results supported the result of the cell parameter measurement. From chemical analysis by energy-dispersive X-ray spectroscopy, Sr was detected overall in the same ratio. the result indicated that Sr substitution was not concentrated but spread overall in the crystals.

From microscopic observation, these crystals were transplant and hexagonal–prismatic in form. Polarizing microscopy, using a 530-nm gypsum plate, revealed the sign of straight extension to be negative. Using an X-ray camera technique, the extended direction was identified as the c-axis. These results pointed out that the crystals were optically uniaxial and negative. This optical character is the same as in other apatite minerals.

Figure 3 shows the infrared spectrum of the single crystals. Absorption bands by HPO_4 were detected at 782, 2084, and 2364 cm^{-1}. The HPO_4 group appeared to be substituted for the PO_4 group in the crystals.

3.2. Crystal Structure Refinement of Sr-Substituted Hydroxyapatite

The 0th and higher layer Weissenberg photographs around the c-axis showed a six-fold symmetry around the c^*-axis and no minor symmetry. Weissenberg photographs around the a-axis revealed a mirror plane perpendicular to the c^*-axis and a symmetric absence for the $(00l)$ $l = 2n$ type. Therefore, the crystal symmetry of Sr-substituted hydroxyapatite was Laue group $6/m$ and space group $P6_3/m$ (centrosymmetric). The crystal data of Sr-substituted hydroxyapatite single crystals are shown in Table 2. In the table, the chemical formula was calculated from chemical analysis data preparing charge balance by H^+ atom, because the existence of an HPO_4 group was detected from the infrared spectrum (Fig. 3). The observed density (3.207(1) g/cm^3) was greater than calculated one (3.149 g/cm^3). This may be due to the underestimation of Sr content in wavelength-dispersive spectroscopic determination. The results of refinement (i) show R = 5.9% and R_w = 6.3% with substitution of Sr only for the Ca(1) site. The results of refinement (ii) were R = 5.9% and R_w = 6.3%; however, the results of refinement (iii) were R = 8.1% and R_w = 8.7%. From the result

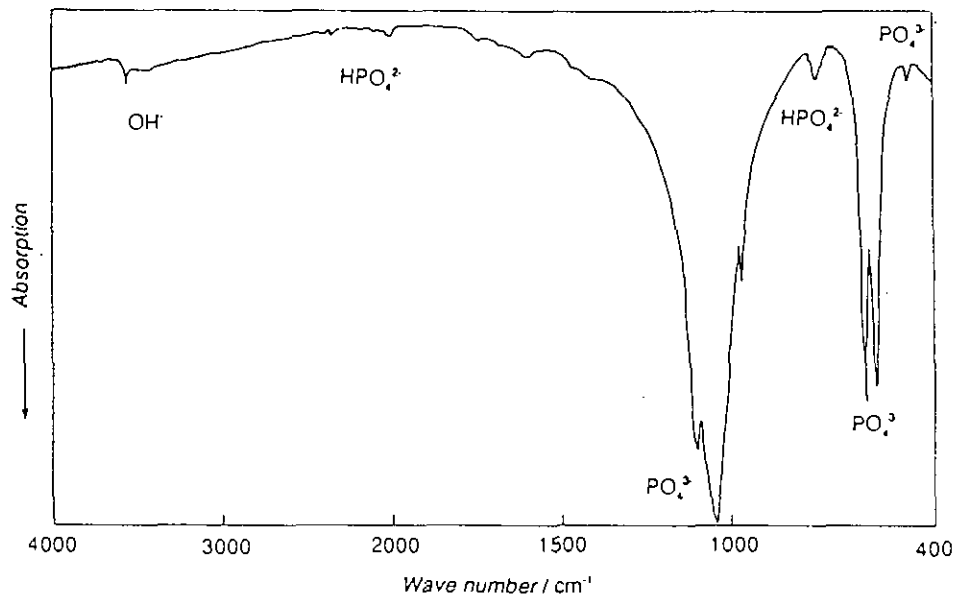

FIG. 3. Infrared spectrum of Sr-substituted hydroxyapatite single crystal grown hydrothermally.

of Hamilton's R-factor significant test (15), R-factors (i) and (ii) were essentially same; however, R-factor (iii) was rejected at the 0.005 level. Further, in procedure (i), the Sr population in the Ca(1) site had a tendency to become greater than the Sr population calculated from chemical analysis of the growing Sr population in the Ca(2) site less than zero; this suggested that the Sr amount calculated by wavelength-dispersive spectroscopy was smaller than the real Sr amount as indicated by observed density. These results indicated that Sr ions were preferentially substituted for the Ca(1) site in the structure of hydrothermally grown Sr-substituted hydroxyapatite and supported the results of Kikuchi *et al.* (6) and Gedalia *et al.* (2). However, this conclusion was contrary to the conclusion of Sudarsanan and Young (7) and Hughes *et al.* (8). In their model, Sr ions were substituted for both the Ca(1) and Ca(2) sites with a preference for Ca(2). The authors assumed that these differences between Sr–chlorapatite flux grown by Sudarsanan and Young (7) and the crystals grown in the present study were due to the conditions of crystal growth; i.e., hydroxyapatite with high crystallinity was permitted to substitute Sr ions along only the Ca(1) channel in aqueous solution.

Table 3 shows the positional and thermal parameters, and Table 4 shows the interatomic distances and bond angles. We considered that insufficiency of positive charge because of cation deficiency was compensated by substitution of the HPO_4 group for the PO_4 group. In Sr-substituted hydroxyapatite, the OH groups were close to the mirror planes compared with Ca–hydroxyapatite (13). Figure 4 shows the crystal structure of Sr-substituted hydroxyapatite projected on the a-plane. In the Sr-substituted hydroxyapatite, the average P–O distance,

TABLE 2
Crystal Data of Sr-Substituted Hydroxyapatite

$Ca_{9.42}Sr_{0.18}H_{0.8}(PO_4)_6(OH)_2$	
F.W.	998.11
a = 9.3920(7) Å	c = 6.890(1) Å
Space group	$P6_3/m$ ($P6_3$)
d_{obs} = 3.207(1) g/cm³	d_x = 3.149 g/cm³
Z = 1	

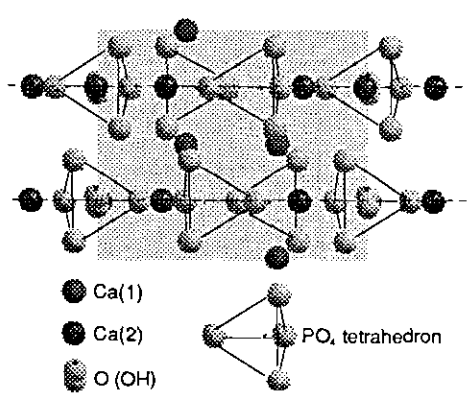

FIG. 4. Crystal structure of Sr-substituted hydroxyapatite projected on the a-plane. The OH groups were slightly close to the mirror plane indicated by dashed lines.

TABLE 3
Population, Positional ($\times 10^4$), Anisotropic Thermal ($\times 10^4$), and Equivalent Thermal Parameters of Sr-Substituted Hydroxyapatite

Atom	Population	x	y	z	U_{11}	U_{22}	U_{33}	U_{12}	U_{13}	U_{23}	B_{eq}
Ca(1)	0.8690(34)	3333	6667	−12(1)	119	119	55	59	0	0	0.77
Sr(1)	0.0456(15)	3333	6667	−12	119	119	55	59	0	0	0.77
Ca(2)	0.9902(24)	2494(1)	75(1)	2500	84	86	74	36	0	0	0.66
P	1.0000	3694(1)	3988(1)	2500	73	63	58	39	0	0	0.50
O(1)	0.9921(148)	4847(3)	3273(3)	2500	139	103	123	90	0	0	0.86
O(2)	1.0000(108)	1206(3)	5340(3)	2500	99	95	216	60	0	0	1.04
O(3)	0.9706(124)	2565(2)	3414(2)	716(3)	274	129	85	133	77	51	1.17
O(H)	1.0000(15)	0	0	2309(30)	108	108	224	54	0	0	1.16

Note. Sr(1) occupy the Ca(1) site in this structure. $B_{eq} = 8/3\pi^2\{U_{11}a^{*2}a^2 + U_{22}b^{*2}b^2 + U_{33} + U_{12}a^*b^*ab \cos\gamma\}$.

1.532 Å, became slightly smaller and the variance of O–P–O bond angles, $\sigma_\theta^2 = 3.63$, became slightly larger than the values, 1.537 Å and 3.36, in Ca-hydroxyapatite (13). The variance, σ_θ^2, is defined as

$$\sigma_\theta^2 = \sum_{i=1}^{6} \frac{(\theta_i - 109.47°)^2}{6},$$

where θ_i is each O–P–O bond angle and 109.47° is the ideal O–P–O bond angle in the PO_4 tetrahedron. Without these delicate differences, the crystal structure of hydrothermally synthesized Sr-substituted hydroxyapatite was, in principle, the same as that of hydroxyapatite. On the other hand, the greatest difference between the present study and that of Sr-bearing fluorapatite (8) was the preferential substitution site of Sr for Ca; however,

TABLE 4
Interatomic Distance and Bond Angle of Sr-Substituted Hydroxyapatite

Symmetry code
(0) x, y, z (i) $y - x, 1 - x, z$ (ii) $x - y, x, z + 1/2$
(iii) $1 - x, 1 - y, 1 - z$ (iv) $x - y, x, 1 - z$ (v) $y - x, 1 - x, 1/2 - z$

	Present work	Hydroxyapatite (13)	Sr–fluorapatite (8)		Present work	Hydroxyapatite (13)
PO_4 tetrahedron						
P–O(1)	1.534(4)	1.539(1)	1.534(2)	O(1)–P–O(2)	111.4(2)	111.13(1)
P–O(2)	1.528(3)	1.539(1)	1.540(2)	O(1)–P–O(3)^{0,iii}	111.2(2)	111.41(4)
P–O(3)	1.534(2)	1.532(1)	1.533(1)	O(2)–P–O(3)^{i,iv}	108.2(1)	107.76(8)
Mean	1.532	1.537	1.535	O(3)–P–O(3)^{iii}	106.5(1)	107.47(5)
Ca(1)–O(1)	2.401(2)	2.405(1)	2.404(1)			
Ca(1)–O(2)	2.459(2)	2.454(1)	2.457(2)			
Ca(1)–O(3)	2.811(2)	2.802(1)	2.810(1)			
Ca(2)–O(1)	2.696(2)	2.710(1)	2.687(2)			
Ca(2)–O(2)	2.383(3)	2.357(1)	2.388(2)			
Ca(2)–O(3)^{ii}	2.357(2)	2.345(2)	2.357(2)			
Ca(2)–O(3)^{v}	2.493(3)	2.511(1)	2.507(1)			
Ca(2)–O(4)	2.311(1)	2.389(1)	2.2991(5)[a]			
Ca(2)–Ca(2)	4.146(1)	4.084(1)				
O(1)–O(2)	2.528(5)	2.538(2)				
O(1)–O(3)^{0,iii}	2.531(4)	2.537(1)				
O(2)–O(3)^{ii,v}	2.480(4)	2.476(1)				
O(3)–O(3)^{iii}	2.458(3)	2.475(2)				

[a] Ca(2)–F length.

the interatomic distance without P–O(2) was similar. Partial or full substitution of Sr for Ca caused lattice expansion (2–6, 16, 17), and whole interatomic distance in the Sr–hydroxyapatite (16) should become larger than Ca–hydroxyapatite; therefore, random substitution of Sr is considered to introduce expansion of whole interatomic distance. However, in the present study and in Hughes *et al.*, some of interatomic distances showed no expansion. This was due to the existence of a preferential substitution site for Sr.

The sequence of hydrothermal growth of Sr-substituted hydroxyapatite was considered as follows. First, Ca–hydroxyapatite crystals were grown under the hydrothermal conditions. After that, Sr ions were substituted for Ca in HAp along the Ca(1) channel only, and Sr-substituted hydroxyapatite having a substitution ratio up to 40 mole% of Sr/(Sr + Ca) formed. On the other hand, Ca ions in the Ca(2) site were considered more table than Sr ions in the Ca(2) site under the hydrothermal conditions, and the Sr substitution ratio was not higher than the mixing ratio of Sr/(Sr + Ca) in starting materials (6). The present results showed that the average Ca(2)–O distance was a little shorter than that of HAp; therefore, ionic bonding strength for Ca(2) ions was considered to increase with Sr substitution.

ACKNOWLEDGEMENTS

The authors are deeply thankful to Dr. Masataka Ohgaki and Dr. Satoshi Nakamura in the Institute for Medical and Dental Engineering, Tokyo Medical and Dental University for their invaluable suggestions and discussions. This study was supported by "Seitai Zairyo Kenkyu-kai" Foundation.

REFERENCES

1. H. Aoki, S. Okayama, K. Kondo, and M. Akao, *Biomed. Mater. Eng.* **3,** 25 (1993).
2. I. Gedalia, D. Almog, and S. Yariv, *Caries Res.* **11,** 287 (1977).
3. R. L. Collin, *J. Am. Chem. Soc.* **81,** 5275 (1959).
4. R. L. Collin, *J. Am. Chem. Soc.* **82,** 5067 (1960).
5. C. Lagergren, and D. Calström, *Acta Chem. Scand.* **11,** 545 (1957).
6. M. Kikuchi, S. Kano, A. Yamazaki, R. Otsuka, M. Oghaki, S. Nakamura, M. Akao, and H. Aoki, *Phosphate Res. Bull.* **1,** 483 (1991).
7. K. Sudarsanan, and R. A. Young, *Acta Crystallogr., Sect. B* **36,** 1525 (1980).
8. J. M. Hughes, M. Cameron, and K. D. Crowley, *Am. Mineral.* **76,** 1857 (1991).
9. T. Sakurai, "UNICS (Universal Crystallographic Computation Program System)." The Crystallographic Society of Japan, Tokyo, 1967.
10. J. A. Ibers, and W. C. Hamilton, "International Tables for X-Ray Crystallography, Vol. IV," p. 71. Kynoch Press, Birmingham, 1974.
11. M. Tokonami, *Acta Crystallogr.* **19,** 486 (1965).
12. T. Fukamachi, *Tech. Rep. ISSP* **B12** (1971).
13. K. Sudarsanan, and R. A. Young, *Acta Crystallogr., Sect. B* **25,** 1534 (1968).
14. P. Coppens, and W. C. Hamilton, *Acta Crystallogr., Sect. A* **26,** 71 (1970).
15. W. C. Hamilton, *Acta Crystallogr.* **18,** 502 (1965).
16. K. Sudarsanan, R. A. Young, *Acta Crystallogr., Sect. B* **28,** 3668 (1972).
17. S. Okayama, M. Akao, S. Nakamura, Y. Shin, M. Higashikata, and H. Aoki, *Biomed. Mater. Eng.* **1,** 13 (1990/91).